Supplementary Information for

Photo-induced ligand release from a silicon phthalocyanine dye conjugated with monoclonal antibodies; A mechanism of cancer cell cytotoxicity after near infrared photoimmunotherapy

Kazuhide Sato, [†,‡,§] Kanta Ando,[¶] Shuhei Okuyama,[†,⊥] Shiho Moriguchi,[⊥] Tairo Ogura,[⊥] Shinichiro Totoki,[⊥] Hirofumi Hanaoka,[†] Tadanobu Nagaya,[†] Ryohei Kokawa,[⊥] Hideo Takakura,[¶] Masayuki Nishimura,[⊥] Yoshinori Hasegawa, [§] Peter L. Choyke,[†] Mikako Ogawa,[¶] and Hisataka Kobayashi[*,†]

[†]Molecular Imaging Program, Center for Cancer Research, National Cancer Institute, National Institutes of Health, Bethesda, Maryland, 20892-1002, USA.
[‡] Institute for Advanced Research, Nagoya University, Nagoya, Aichi, 464-0814, Japan
[§] Department of Respiratory Medicine, Nagoya University Graduate School of Medicine, Nagoya, Aichi, 466-8550, Japan
[¶]Laboratory for Bioanalysis and Molecular Imaging, Graduate School of Pharmaceutical Sciences, Hokkaido University, Sapporo, Hokkaido, 060-0812, Japan.
[⊥] Shimadzu Corporation, Kyoto, 604-8511, Japan

Correspondence should be addressed to: Hisataka Kobayashi, M.D., Ph.D.
Molecular Imaging Program, Center for Cancer Research, National Cancer Institute, NIH, Building 10, Room B3B69, MSC1088, Bethesda, MD 20892-1088.
Phone: 240-858-3069; Fax: 240-541-4527; E-mail: kobayash@mail.nih.gov

Supplementary Figure1

a

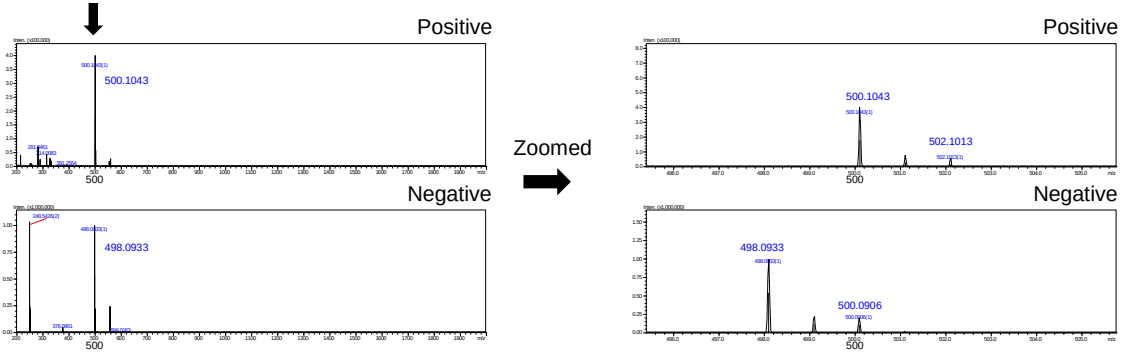

b

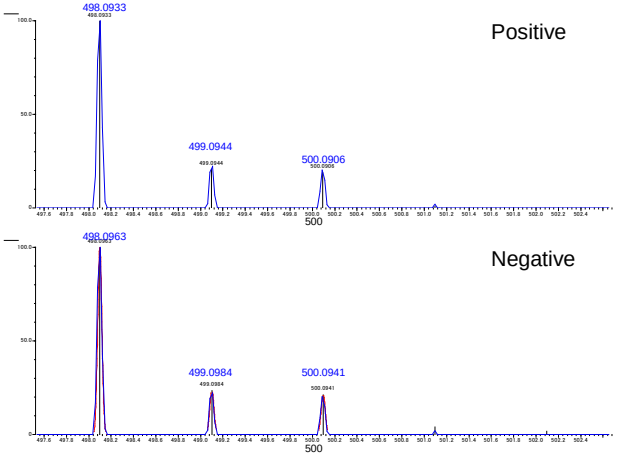

$C_{14}H_{34}NO_{10}S_3Si$ (+1)
Exact Mass: 500.111418
$C_{14}H_{33}NO_{10}S_3Si$ (0)
Exact Mass: 499.103593
$C_{14}H_{32}NO_{10}S_3Si$ (-1)
Exact Mass: 498.095768
$C_{14}H_{31}NO_{10}S_3Si$ (-2)
Exact Mass: 497.087943

Figure. S1. Ligand release from IR700-dye with NIR-light irradiation was further analyzed to detect isotope peak.

(a) Analysis of isotope peak. (b) Structure prediction on Molecular weight was performed and $C_{14}H_{34}NO_{10}S_3Si$ was predicted as released ligand.

Supplementary Figure2

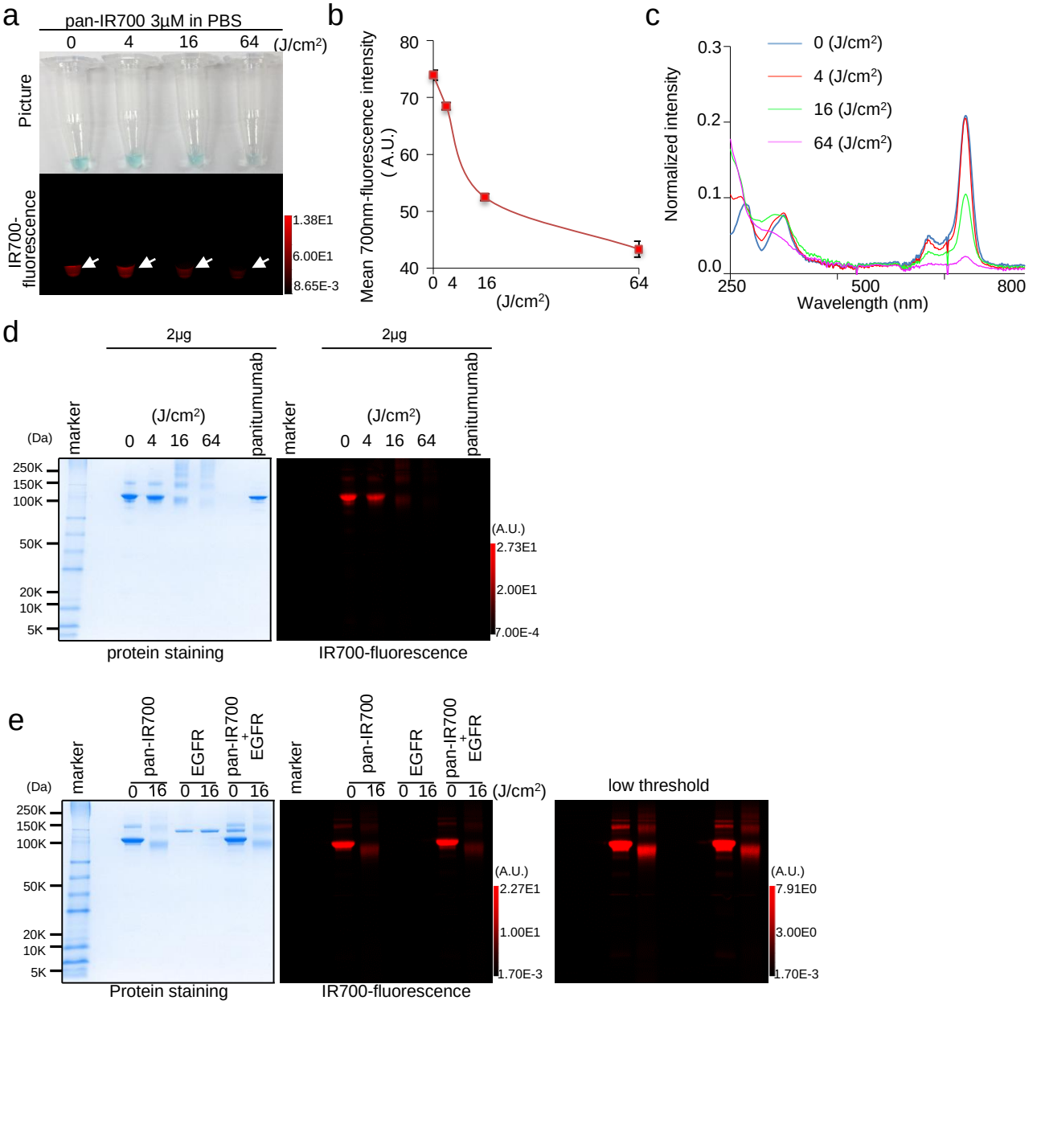

Figure. S2. The releasing ligand of pan-IR700 with NIR-light induced panitumumab into hydrophobic to make aggregations, which also make aggregation to their antigen, EGFR protein.

(a) 3 mM pan-IR700 in PBS was irradiated with NIR-light, and imaged with white light and 700 nm-fluorescence. Both the blue color in the tube and the 700 nm-fluorescence decreased in a light dose dependent manner. (b) Mean 700 nm-fluorescence intensity of pan-IR700 in PBS was decreased in a dose dependent manner (n = 3). (c) Absorbance profile of pan-IR700 in PBS with NIR-light irradiation showed decrease of the absorbance at Q band at 690 nm of the SiPcs. (d) SDS-PAGE of NIR-light irradiated pan-IR700 revealed the protein-band of panitumumab disappeared in a dose-dependent manner, and some bands over panitumumab increased with smear. The IR700-fluorecence in the SDS-PAGE decreased in a light-dose dependent manner. (e) The complex of pan-IR700 and recombinant EGFR protein was irradiated with NIR-light and electrophoresed by SDS-PAGE. The protein bands of not only pan-IR700 but also EGFR become thin with smear over its protein band along with loss of IR700-fluorescence.

Supplementary Figure3

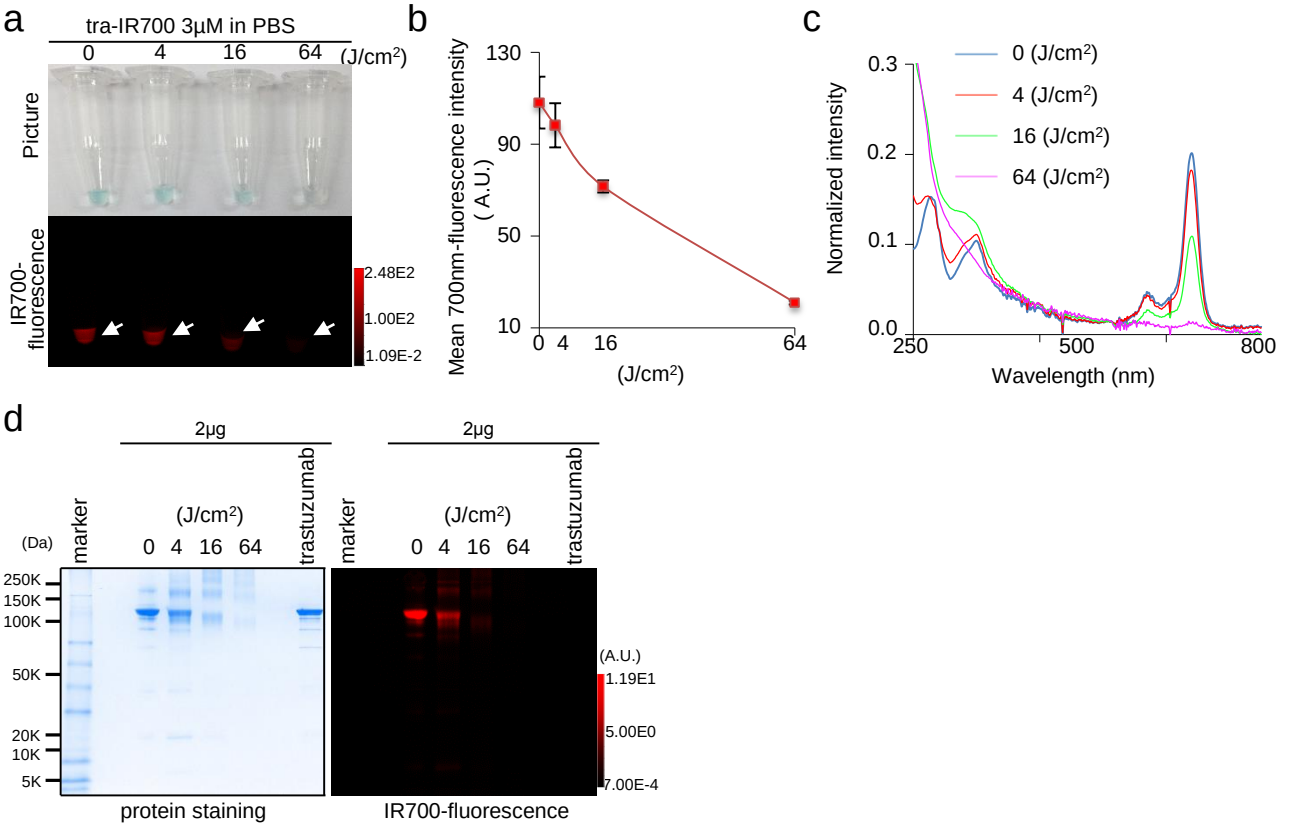

Figure. S3. Tra-IR700 with NIR-light irradiation also made aggregation with loss of IR700-fluorescence.

(a) 3 mM tra-IR700 in PBS was irradiated with NIR-light, and imaged with white light and 700 nm-fluorescence. Both the blue color in the tube and the 700 nm-fluorescence decreased in a light dose dependent manner. (b) Mean 700 nm-fluorescence intensity of tra-IR700 in PBS was decreased in a dose dependent manner (n = 3). (c) Absorbance profile of tra-IR700 in PBS with NIR-light irradiation showed decrease of the absorbance at Q band at 690 nm of the silicon phtalocyanines (SiPcs). (d) SDS-PAGE of NIR-light irradiated tra-IR700 revealed the protein-band of trastuzumab disappeared in a dose-dependent manner, and some bands over trastuzumab increased with smear. The IR700-fluorecence in the SDS-PAGE decreased in a light-dose dependent manner.

Supplementary Figure4

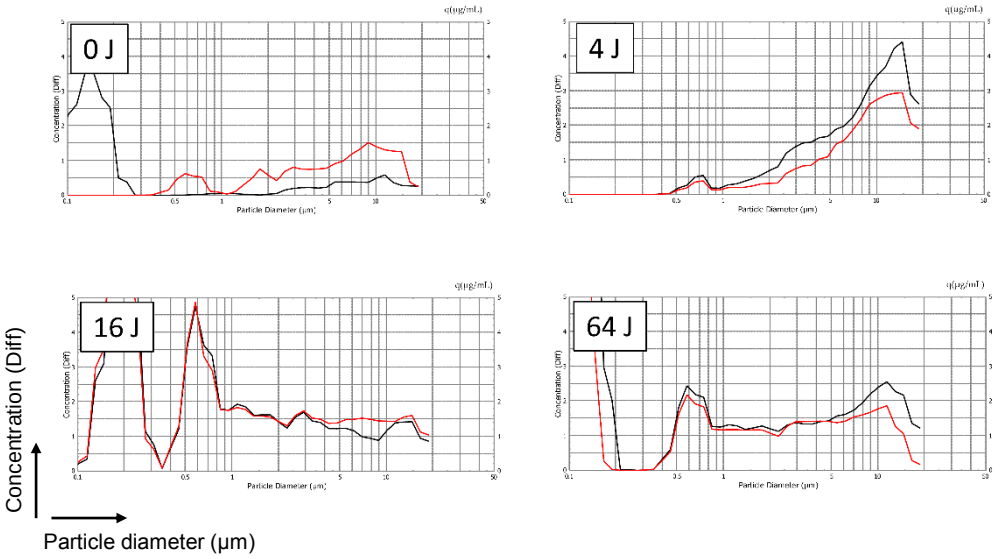

Figure. S4. Distribution of the particles of aggregated cet-IR700.

Distribution of the particles of aggregated cet-IR700 was showed as a graph. Total particles in 64 J/cm^2 decreased, suggesting the particles become hydrophobic.

Supplementary Figure5

a

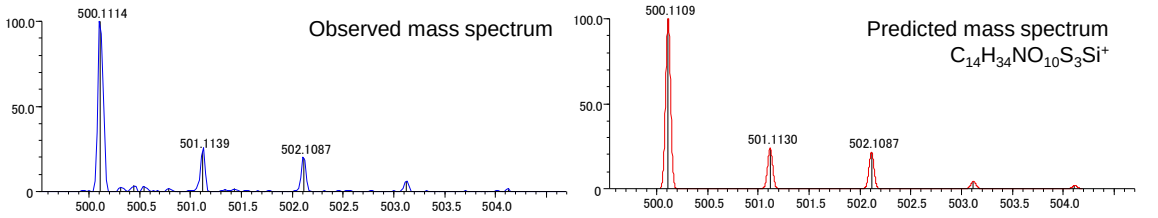

b

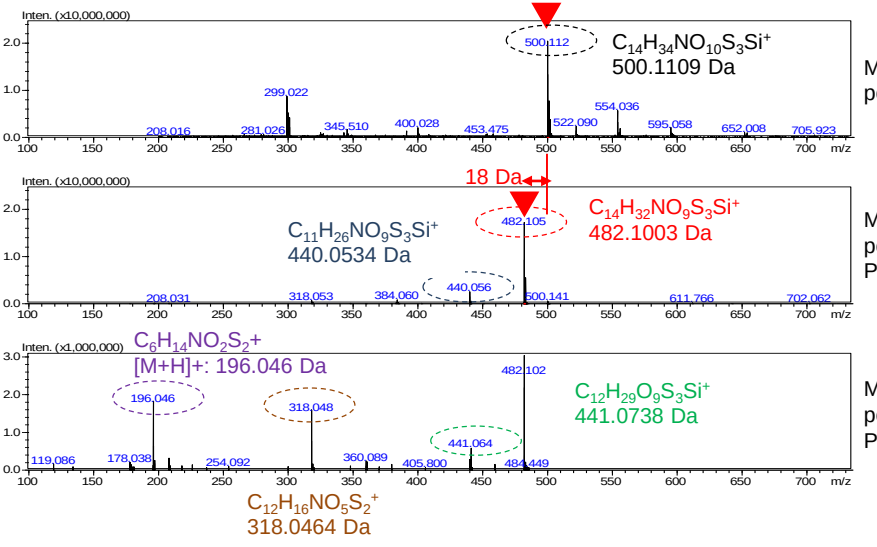

c

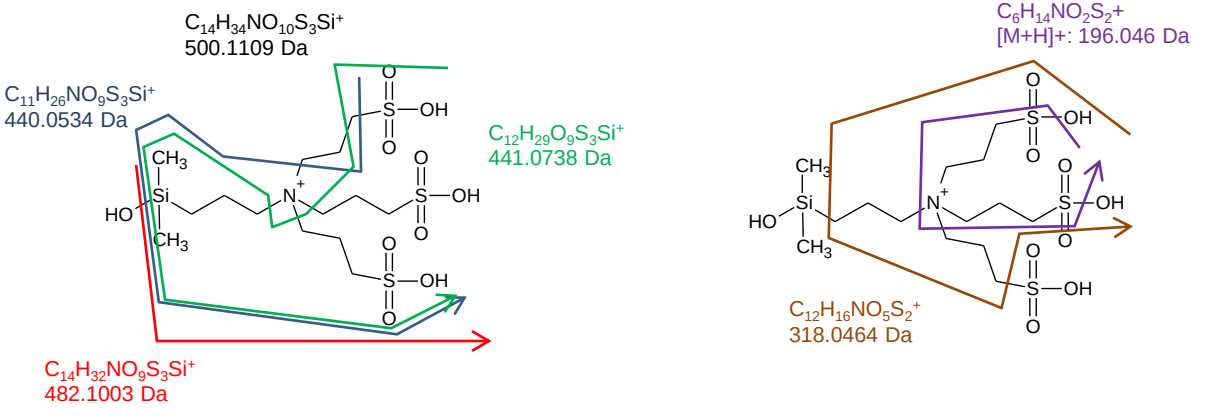

Figure. S5. Ligand release from cet-IR700 with NIR-light irradiation was further confirmed with product-scan and fragmentation by IT-TOF-MS.

(a) Result of product-scan method in IT-TOF MS. (b) Mass spectra of the released ligand from cet-IR700 after further fragmentation confirmed the detected peak as $C_{14}H_{34}NO_{10}S_3Si$. (c) Suggested fragmentation of the ligand detected in the mass spectra (panel b).

Supplementary Figure6

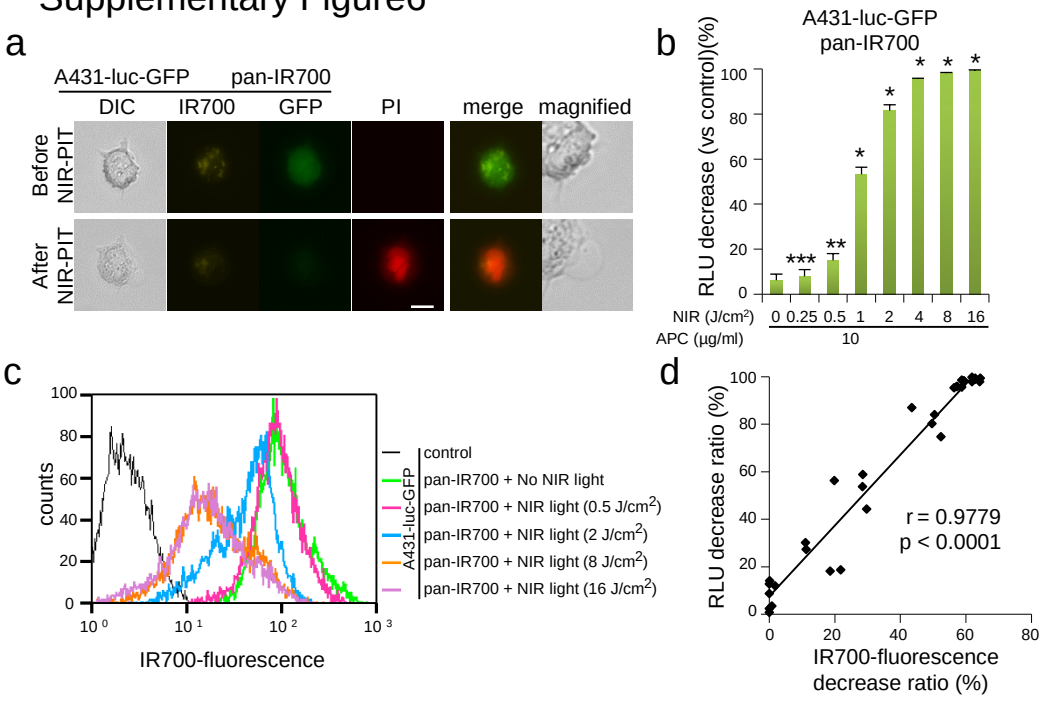

Figure. S6. NIR-PIT cell death in vitro was detected as the loss of IR700-fluorescence (A431-luc-GFP with pan-IR700)

(a) A431-luc-GFP cells were incubated with pan-IR700 for 6 hr, and observed with a microscope before and after irradiation of NIR-light (2 J/cm^2). Necrotic cell death with loss of IR700-fluorescence was observed after exposure to NIR-light (1 hr after NIR-PIT). Bar = 50 μm. (b) Luciferase activity in A431-luc-GFP cells was measured as percentage decrease in relative light units (RLU) vs untreated cells, which decreased in a NIR-light dose-dependent manner. (n = 4, *p < 0.0001, **p < 0.001, ***p < 0.01, vs. untreated control, Student's t test) (c) IR700-fluorescence of a cell treated with NIR-PIT, was evaluated with a flow cytometry and shows decreased fluorescence in a NIR-light dose-dependent manner. (d) Positive correlation between RLU decrease ratio and IR700-fluorescence decrease ratio (n = 30, r = 0.9779, p < 0.0001, Pearson's product moment correlation coefficient).

Supplementary Figure7

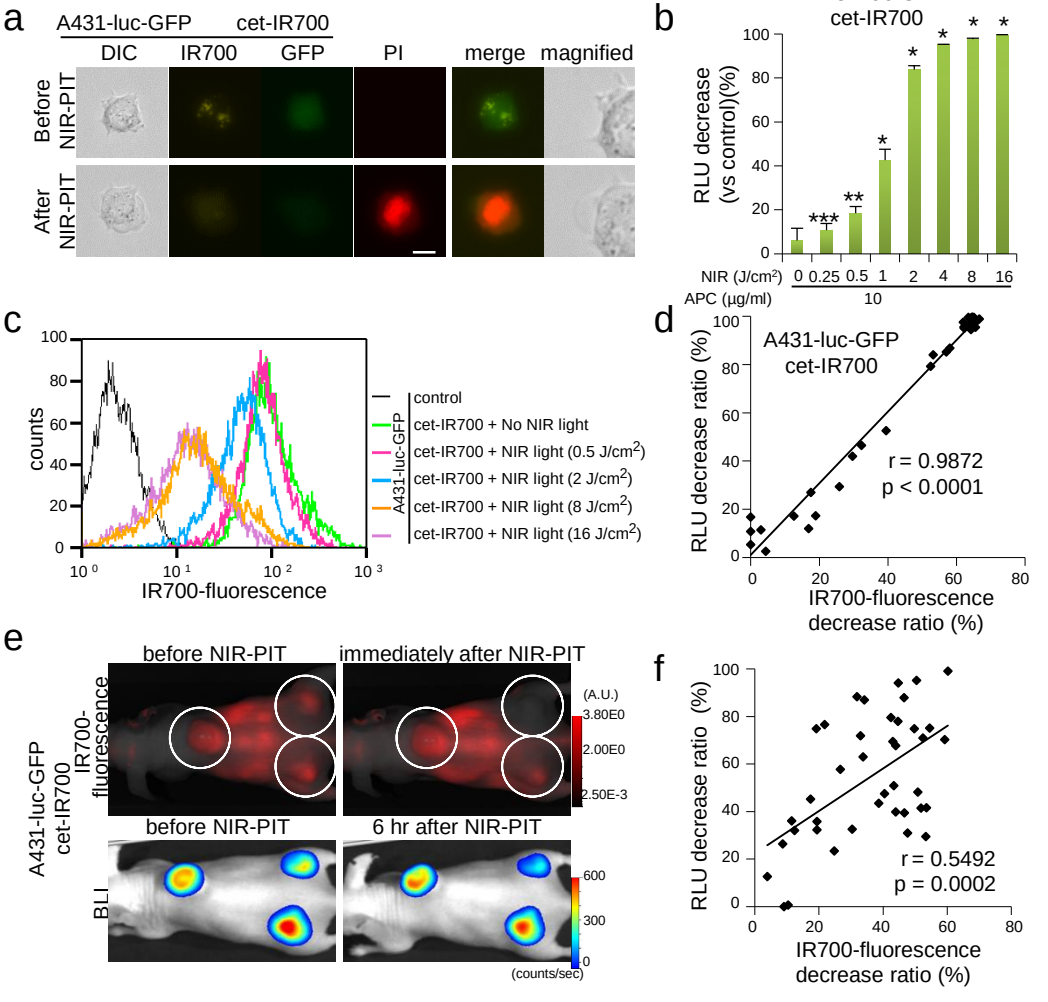

Figure. S7. Correlation between loss of IR700-fluorescence and antitumor effect in vitro and in vivo (A431-luc-GFP with cet-IR700)

(a) A431-luc-GFP cells were incubated with cet-IR700 for 6 hr, and observed with a microscope before and after irradiation of NIR-light (2 J/cm^2). Necrotic cell death with loss of IR700-fluorescence on the cell was observed after exposure to NIR-light (1 hr after NIR-PIT). Bar = 50 μm. (b) Luciferase activity in A431-luc-GFP cells was measured as percentage decrease on relative light unit (RLU) vs untreated cells, which decreased in a NIR-light dose-dependent manner. ($n = 4$, $^*p < 0.0001$, $^{**}p < 0.001$, $^{***}p < 0.01$, vs. untreated control, Student's t test) (c) IR700-fluorescence on the cell treated with NIR-PIT, was evaluated with a flowcytometry and decreased in a NIR-light dose-dependent manner. (d) Positive correlation was detected between RLU decrease ratio and IR700-fluorescence decrease ratio ($n = 30$, $r = 0.9872$, $p < 0.0001$, Pearson's product moment correlation coefficient).(e) *In vivo* BLI and IR700-fluorescence imaging of subcutaneous tumor model before and at 6 hr after the NIR-light irradiation. (f) Positive correlation was detected between RLU decrease ratio and IR700-fluorescence decrease ratio ($n = 40$, $r = 0.5492$, $p = 0.0002$, Peason's product moment correlation coefficient).

Supplementary Figure8

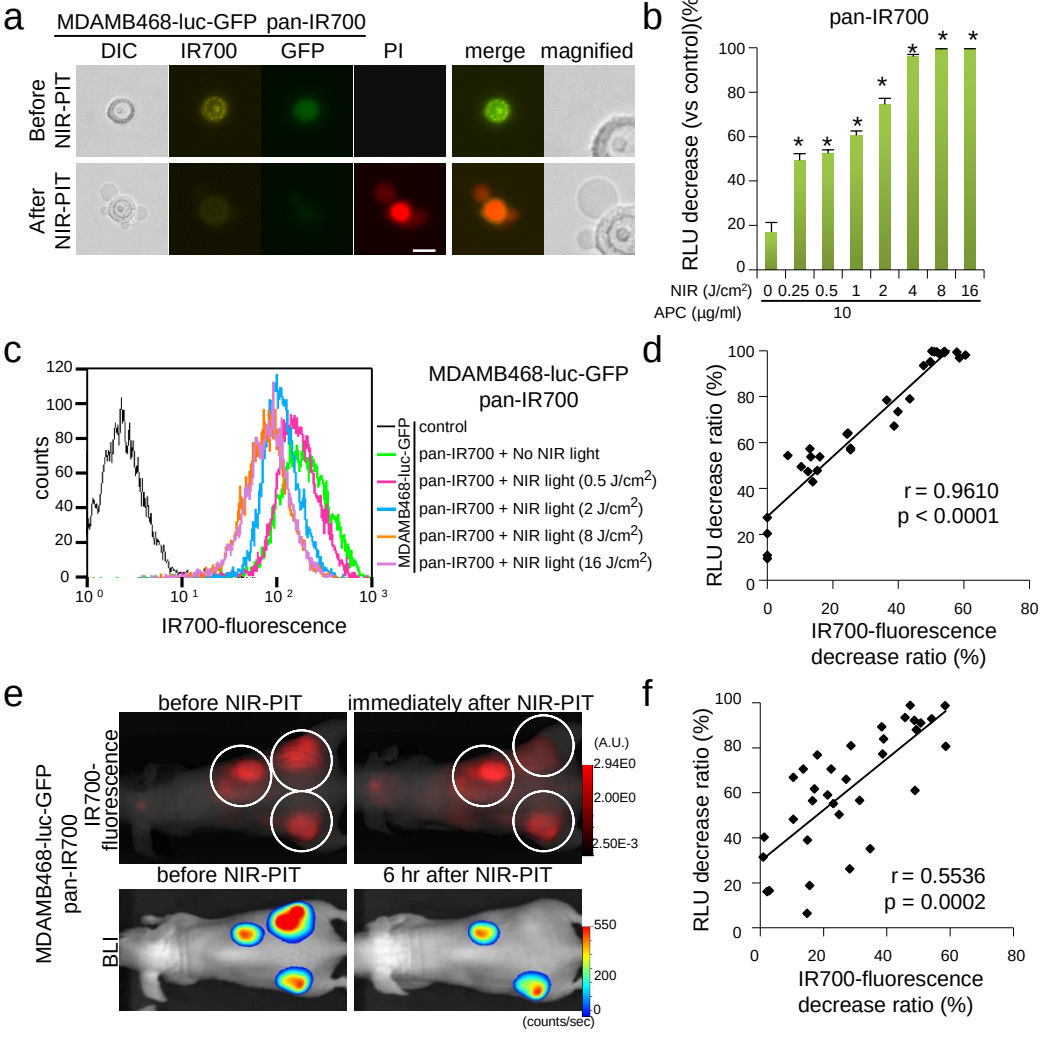

Figure. S8. Correlation between loss of IR700-fluorescence and antitumor effect in vitro and in vivo (MDAMB468-luc-GFP with pan-IR700)

(a) MDAMB468-luc-GFP cells were incubated with pan-IR700 for 6 hr, and observed with a microscope before and after irradiation of NIR-light (2 J/cm^2). Necrotic cell death with loss of IR700-fluorescence was observed after exposure to NIR-light (1 hr after NIR-PIT). Bar = 50 μm. (b) Luciferase activity in MDAMB468-luc-GFP cells was measured as percentage decrease of relative light units (RLU) vs untreated cells, which decreased in a NIR-light dose-dependent manner. ($n = 4$, $^*p < 0.0001$, $^{**}p < 0.001$, $^{***}p < 0.01$, vs. untreated control, Student's t test) (c) IR700-fluorescence in a cell treated with NIR-PIT, was evaluated with a flow cytometry and decreased in a NIR-light dose-dependent manner. (d) Positive correlation was detected between RLU decrease ratio and IR700-fluorescence decrease ratio ($n = 30$, $r = 0.9610$, $p < 0.0001$, Pearson's product moment correlation coefficient).(e) *In vivo* BLI and IR700-fluorescence imaging of subcutaneous tumor model before and at 6 hr after the NIR-light irradiation. (f) Positive correlation was detected between RLU decrease ratio and IR700-fluorescence decrease ratio ($n = 40$, $r = 0.5536$, $p = 0.0002$, Pearson's product moment correlation coefficient).

Supplementary Figure9

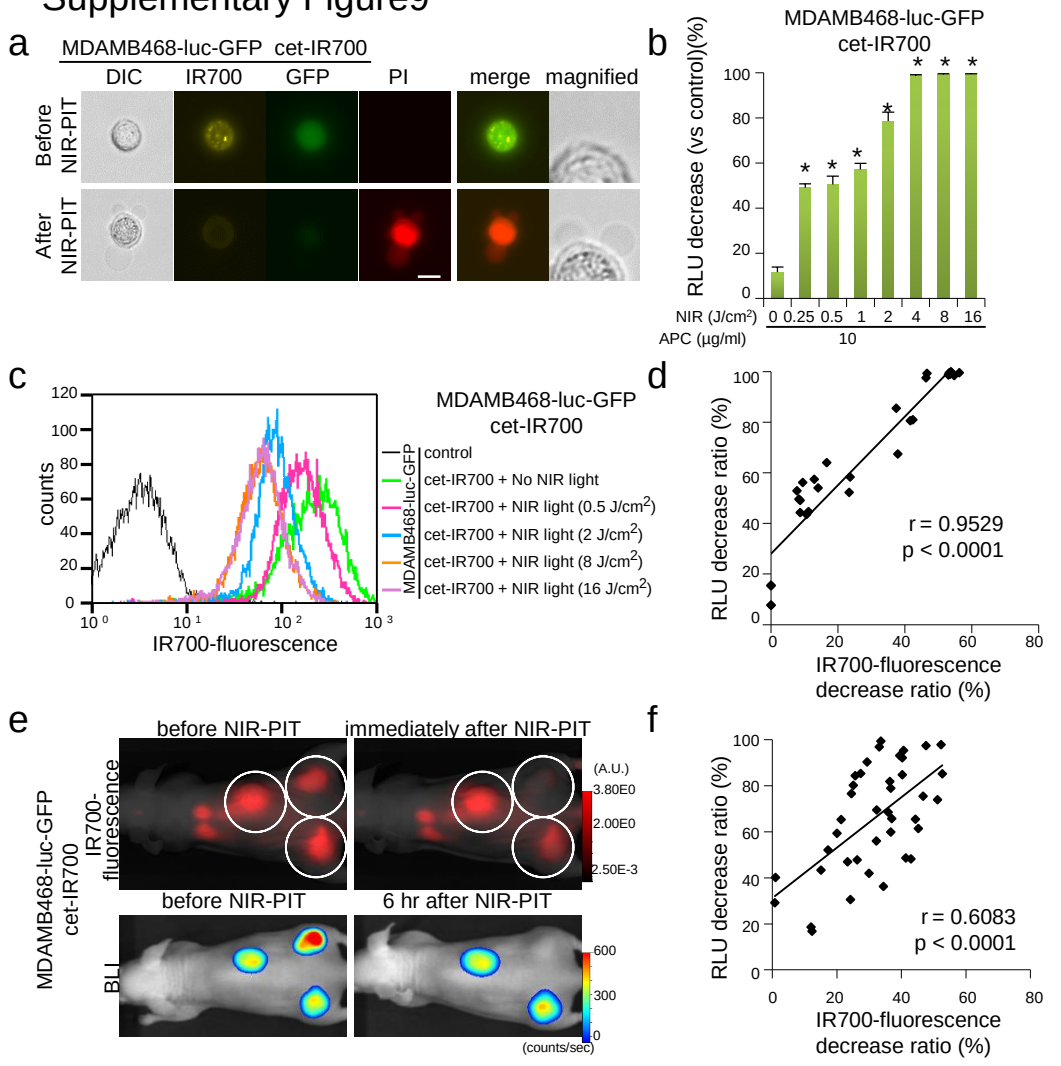

Figure. S9. Correlation between loss of IR700-fluorescence and antitumor effect in vitro and in vivo (MDAMB468-luc-GFP with cet-IR700)

(a) MDAMB468-luc-GFP cells were incubated with cet-IR700 for 6 hr, and observed with a microscope before and after irradiation of NIR-light (2 J/cm^2). Necrotic cell death with loss of IR700-fluorescence was observed after exposure to NIR-light (1 hr after NIR-PIT). Bar = 50 μm. (b) Luciferase activity in MDAMB468-luc-GFP cells was measured as percentage decrease of relative light units (RLU) vs untreated cells, which decreased in a NIR-light dose-dependent manner. ($n = 4$, $^*p < 0.0001$, $^{**}p < 0.001$, $^{***}p < 0.01$, vs. untreated control, Student's t test) (c) IR700-fluorescence on the cell treated with NIR-PIT, was evaluated with a flow cytometry and decreased in a NIR-light dose-dependent manner. (d) Positive correlation was detected between RLU decrease ratio and IR700-fluorescence decrease ratio ($n = 30$, $r = 0.9529$, $p < 0.0001$, Pearson's product moment correlation coefficient).(e) *In vivo* BLI and IR700-fluorescence imaging of subcutaneous tumor model before and at 6 hr after the NIR-light irradiation. (f) Positive correlation was detected between RLU decrease ratio and IR700-fluorescence decrease ratio ($n = 40$, $r = 0.6083$, $p < 0.0001$, Pearson's product moment correlation coefficient).

Supplementary Figure10

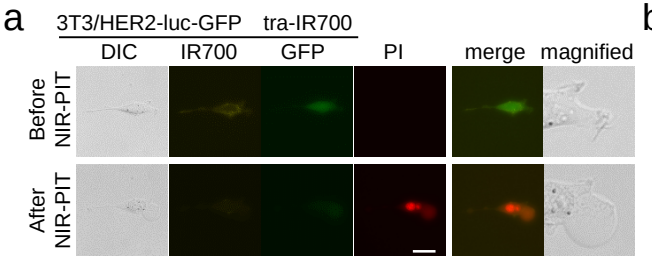

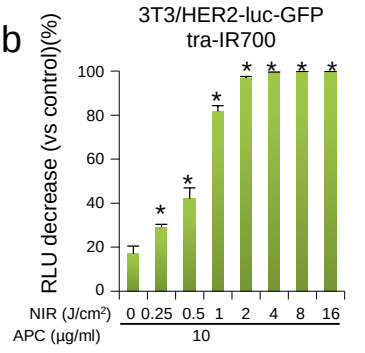

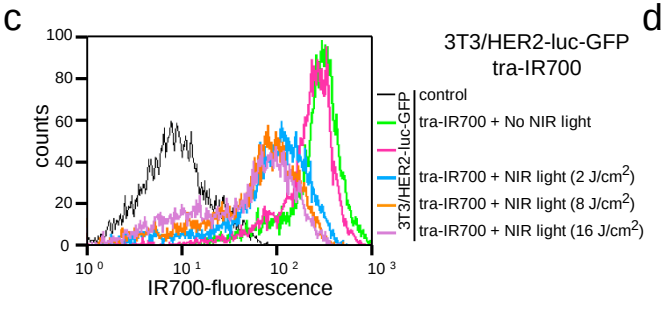

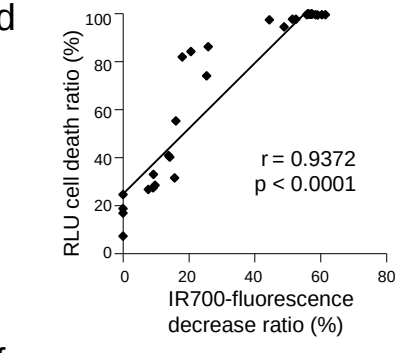

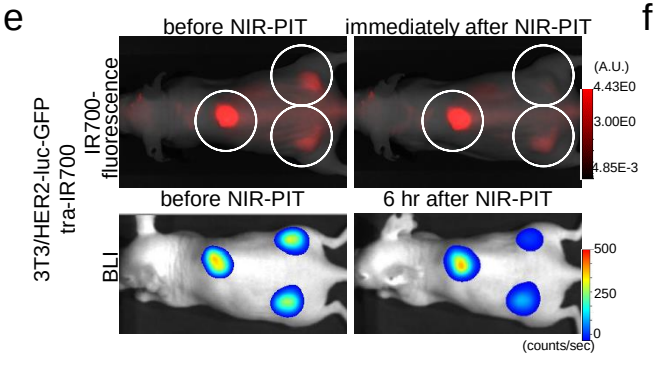

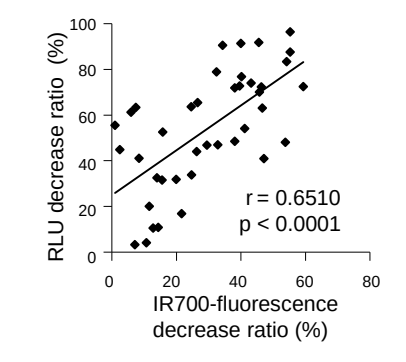

Figure. S10. Correlation between loss of IR700-fluorescence and antitumor effect in vitro and in vivo (3T3/Her2-luc-GFP with tra-IR700)

(a) 3T3/Her2-luc-GFP cells were incubated with tra-IR700 for 6 hr, and observed with a microscope before and after irradiation of NIR-light (2 J/cm^2). Necrotic cell death with loss of IR700-fluorescence was observed after exposure to NIR-light (1 hr after NIR-PIT). Bar = 50 μm. (b) Luciferase activity in 3T3/Her2-luc-GFP cells was measured as percentage decrease of relative light units (RLU) vs untreated cells, which decreased in a NIR-light dose-dependent manner. ($n = 4$, $^*p < 0.0001$, $^{**}p < 0.001$, $^{***}p < 0.01$, vs. untreated control, Student's t test) (c) IR700-fluorescence on the cell treated with NIR-PIT, was evaluated with a flow cytometry and decreased in a NIR-light dose-dependent manner. (d) Positive correlation was detected between RLU decrease ratio and IR700-fluorescence decrease ratio ($n = 30$, $r = 0.9372$, $p < 0.0001$, Pearson's product moment correlation coefficient).(e) *In vivo* BLI and IR700-fluorescence imaging of subcutaneous tumor model before and at 6 hr after the NIR-light irradiation. (f) Positive correlation was detected between RLU decrease ratio and IR700-fluorescence decrease ratio ($n = 40$, $r = 0.6510$, $p < 0.0001$, Pearson's product moment correlation coefficient).

Supplementary Figure11

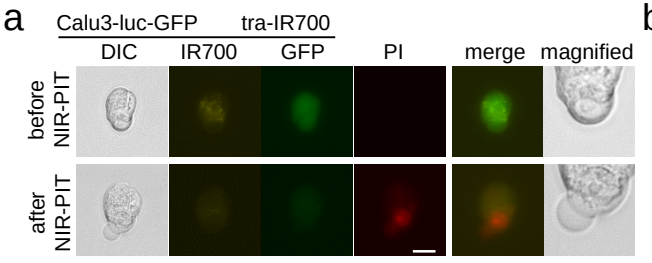

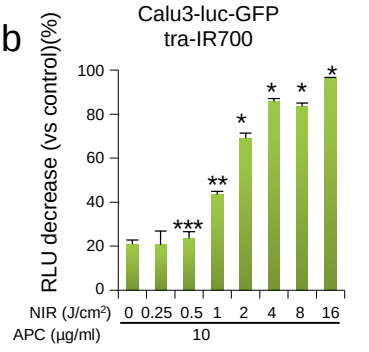

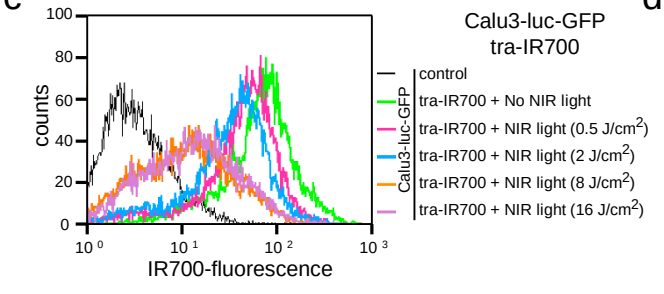

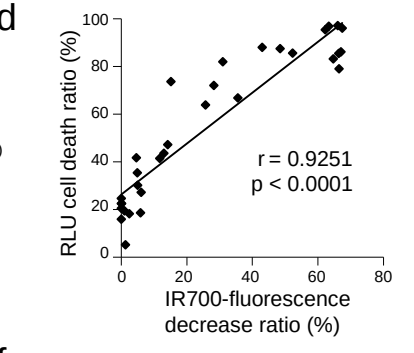

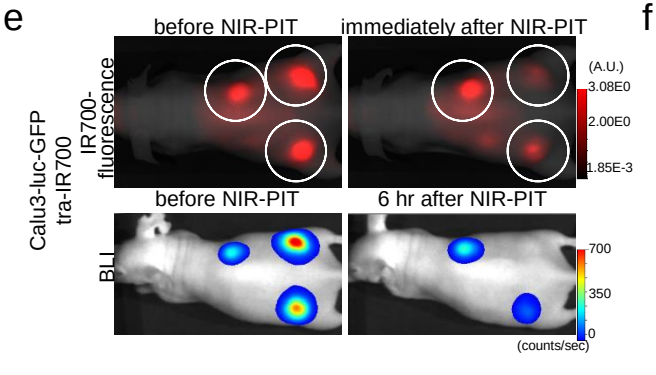

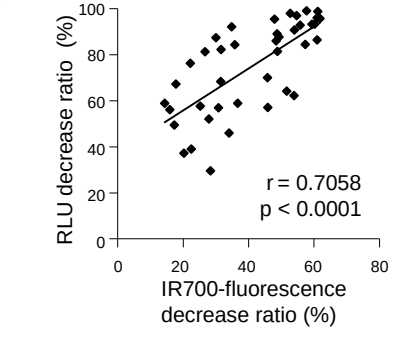

Figure. S11. Correlation between loss of IR700-fluorescence and antitumor effect in vitro and in vivo (Calu3-luc-GFP with tra-IR700)

(a) Calu3-luc-GFP cells were incubated with tra-IR700 for 6 hr, and observed with a microscope before and after irradiation of NIR-light (2 J/cm^2). Necrotic cell death with loss of IR700-fluorescence was observed after exposure to NIR-light (1 hr after NIR-PIT). Bar = 50 μm. (b) Luciferase activity in Calu3-luc-GFP cells was measured as percentage decrease of relative light units (RLU) vs untreated cells, which decreased in a NIR-light dose-dependent manner. ($n = 4$, $^*p < 0.0001$, $^{**}p < 0.001$, $^{***}p < 0.01$, vs. untreated control, Student's t test) (c) IR700-fluorescence of the cell treated with NIR-PIT, was evaluated with a flow cytometry and decreased in a NIR-light dose-dependent manner. (d) Positive correlation was detected between RLU decrease ratio and IR700-fluorescence decrease ratio ($n = 30$, $r = 0.9251$, $p < 0.0001$, Pearson's product moment correlation coefficient). (e) *In vivo* BLI and IR700-fluorescence imaging of subcutaneous tumor model before and at 6 hr after the NIR-light irradiation. (f) Positive correlation was detected between RLU decrease ratio and IR700-fluorescence decrease ratio ($n = 40$, $r = 0.7058$, $p < 0.0001$, Pearson's product moment correlation coefficient).

Supplementary Figure12

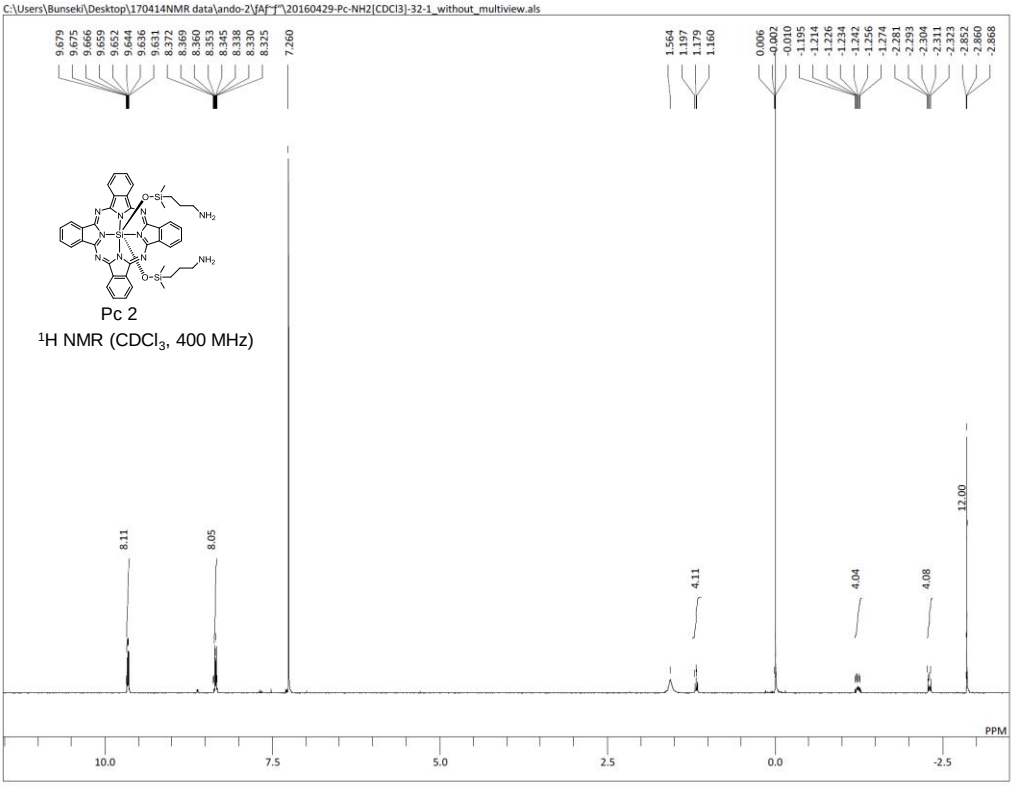

Figure. S12. ^{1}H NMR spectrum of Pc 2 in $CDCl_3$

Supplementary Figure13

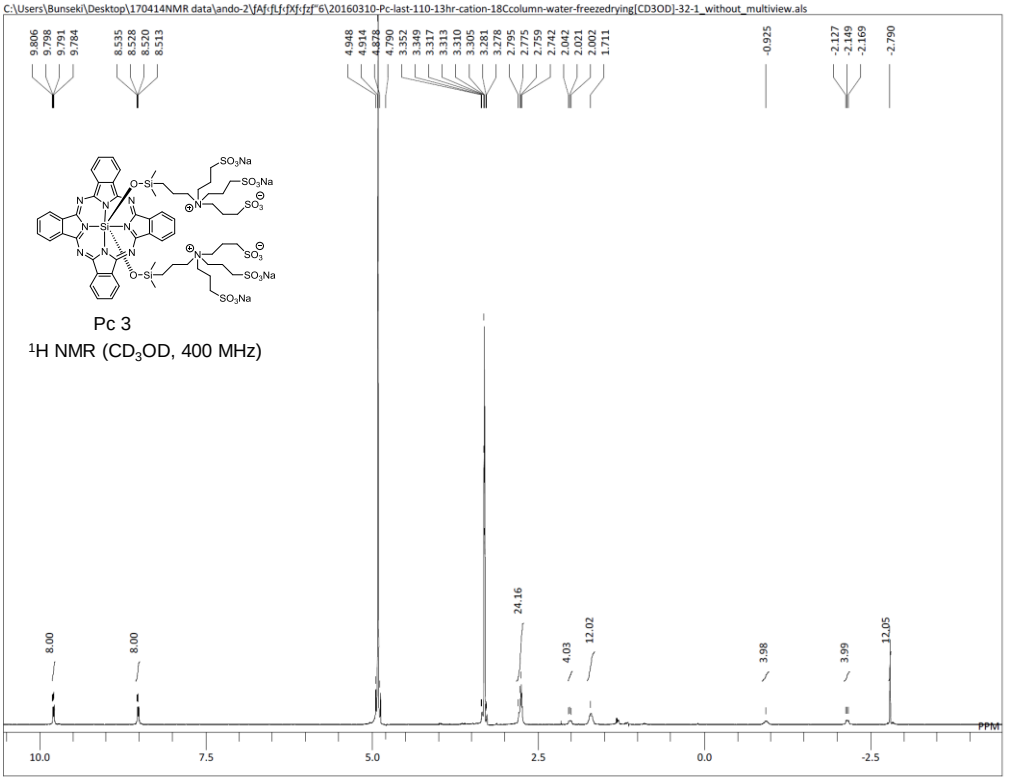

Figure. S13. ^{1}H NMR spectrum of Pc 3 in CD_3OD

Supplementary Figure14

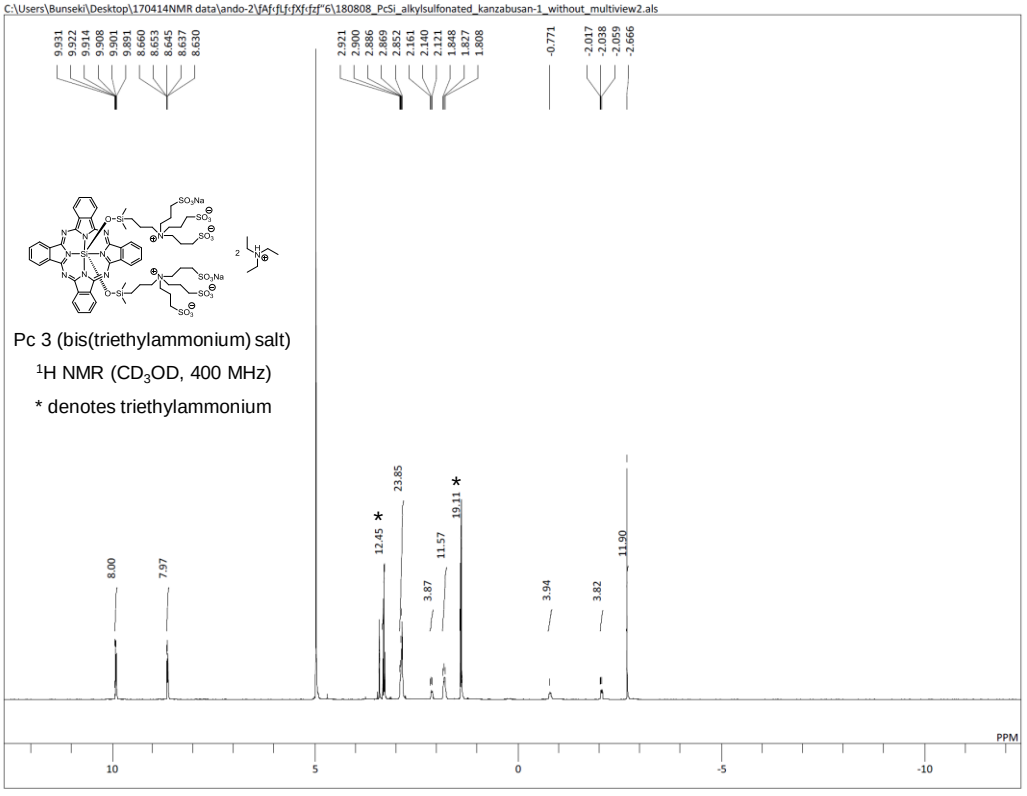

Figure. S14. ^{1}H NMR spectrum of Pc 3 (bis(triethylammonium) salt) in CD_3OD

Pc 3 was not dissolved in CD_3OD so much and the intensity of NMR signal was not enough to confirm the purity. On the other hand, the solubility of the triethylammonium salt was better, so the NMR spectrum is shown as well.

Supplementary Figure15

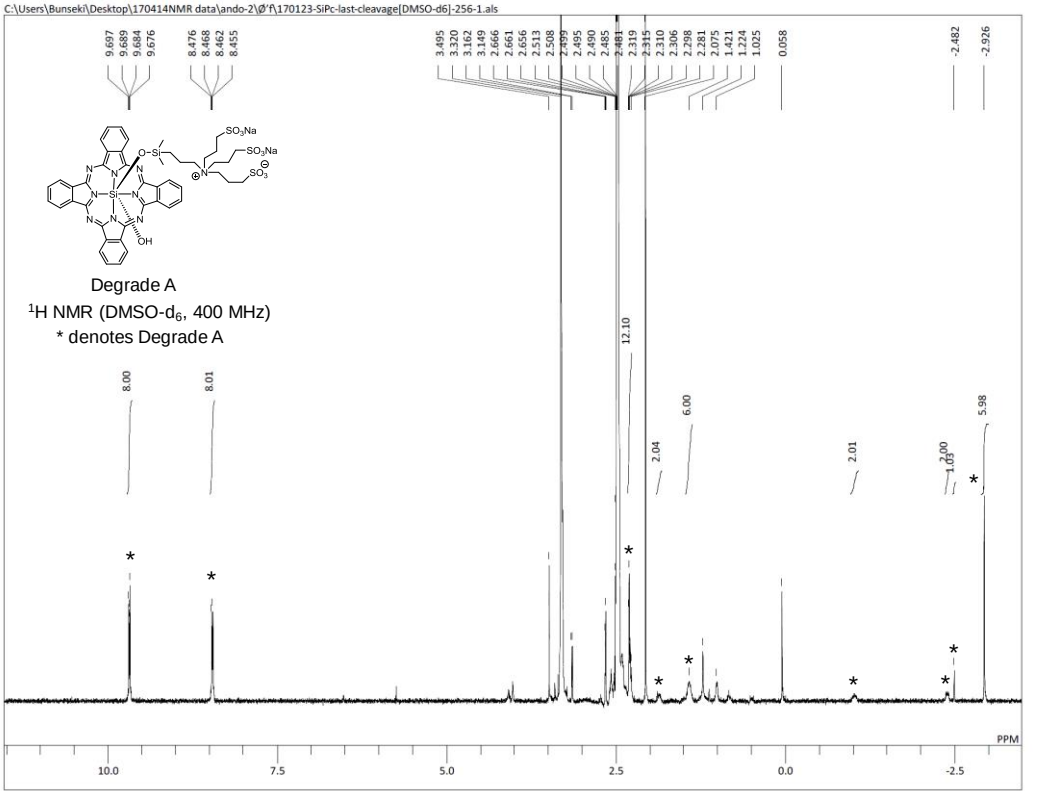

Figure. S15. ^{1}H NMR spectrum of Degrade A in DMSO-d_6

Supplementary video1. 2 .3

Quantitative phase microscope (QPM) and dual-angle selective plane illumination microscope (diSPIM) showd morphological changes of NIR-PIT treated cells.